Vaccination with SARS-CoV-2 Spike Protein and AS03 Adjuvant Induces Rapid Anamnestic Antibodies in the Lung and Protects Against Virus Challenge in Nonhuman Primates

Joseph R. Francica[1], Barbara J. Flynn[1], Kathryn E. Foulds[1], Amy T. Noe[1], Anne P. Werner[1], Ian N. Moore[1], Matthew Gagne[1], Timothy S. Johnston[1], Courtney Tucker[1], Rachel L. Davis[1], Britta Flach[1], Sarah O'Connell[1], Shayne F. Andrew[1], Evan Lamb[1], Dillon R. Flebbe[1], Saule T. Nurmukhambetova[1], Mitzi M. Donaldson[1], John-Paul M. Todd[1], Alex Lee Zhu[2,3], Caroline Atyeo[2,4], Stephanie Fischinger[2,3], Matthew J Gorman[2], Sally Shin[2], Venkata Viswanadh Edara[5,6,7], Katharine Floyd[5,6,7], Lilin Lai[5,6,7], Alida Tylor[1], Elizabeth McCarthy[1], Valerie Lecouturier[8], Sophie Ruiz[8], Catherine Berry[8], Timothy Tibbitts[9], Hanne Andersen[10], Anthony Cook[10], Alan Dodson[10], Laurent Pessaint[10], Alex Van Ry[10], Marguerite Koutsoukos[11], Cindy Gutzeit[12], I-Ting Teng[1], Tongqing Zhou[1], Dapeng Li[13], Barton F. Haynes[13], Peter D. Kwong[1], Adrian McDermott[1], Mark G. Lewis[10], Tong Ming Fu[9], Roman Chicz[9], Robbert van der Most[12], Kizzmekia S. Corbett[1], Mehul S. Suthar[5,6,7], Galit Alter[2], Mario Roederer[1], Nancy J. Sullivan[1], Daniel C. Douek[1], Barney S. Graham[1], Danilo Casimiro[9], and Robert A. Seder[1*]

[1] *Vaccine Research Center, National Institute of Allergy and Infectious Diseases, National Institutes of Health, Bethesda, MD, USA*
[2] *Ragon Institute of MGH, MIT, and Harvard, Cambridge, MA 02139, USA*
[3] *PhD program in Immunology and Virology, University of Duisburg-Essen, Essen, Germany*
[4] *PhD program in Virology, Division of Medical Sciences, Harvard University, Boston, MA, USA*
[5] *Centers for Childhood Infections and Vaccines; Children's Healthcare of Atlanta and Emory University, Department of Pediatrics, Atlanta, GA, 30329, USA*
[6] *Emory Vaccine Center, Emory University School of Medicine, Atlanta, GA 30329, USA*
[7] *Yerkes National Primate Research Center, Atlanta, GA 30329, USA*
[8] *Sanofi Pasteur, Marcy l'Etoile, France*
[9] *Sanofi Pasteur, 38 Sidney Street, Cambridge, MA 02139, USA*
[10] *Bioqual, Inc., Rockville, MD, USA*
[11] *GSK, Wavre, Belgium*
[12] *GSK, Rixensart, Belgium*
[13] *Duke Human Vaccine Institute, Duke University, Durham, NC 27708, USA*

* Corresponding author
Cellular Immunology Section
Vaccine Research Center
National Institute of Allergy and Infectious Disease
National Institutes of Health
40 Convent Drive, MSC 3025, Building 40, Room 3512
Bethesda, MD 20892
E-mail address: rseder@mail.nih.gov

Abstract

Adjuvanted soluble protein vaccines have been used extensively in humans for protection against various viral infections based on their robust induction of antibody responses. Here, soluble prefusion-stabilized spike trimers (preS dTM) from the severe acute respiratory syndrome coronavirus (SARS-CoV-2) were formulated with the adjuvant AS03 and administered twice to nonhuman primates (NHP). Binding and functional neutralization assays and systems serology revealed that NHP developed AS03-dependent multi-functional humoral responses that targeted multiple spike domains and bound to a variety of antibody F_C receptors mediating effector functions *in vitro*. Pseudovirus and live virus neutralizing IC_{50} titers were on average greater than 1000 and significantly higher than a panel of human convalescent sera. NHP were challenged intranasally and intratracheally with a high dose ($3x10^6$ PFU) of SARS-CoV-2 (USA-WA1/2020 isolate). Two days post-challenge, vaccinated NHP showed rapid control of viral replication in both the upper and lower airways. Notably, vaccinated NHP also had increased spike-specific IgG antibody responses in the lung as early as 2 days post challenge. Moreover, vaccine-induced IgG mediated protection from SARS-CoV-2 challenge following passive transfer to hamsters. These data show that antibodies induced by the AS03-adjuvanted preS dTM vaccine are sufficient to mediate protection against SARS-CoV-2 and support the evaluation of this vaccine in human clinical trials.

Introduction

The 2019 outbreak of coronavirus disease (COVID-19) caused by the novel severe acute respiratory syndrome coronavirus (SARS-CoV-2) has become a global pandemic with 112,849,164 infections and 2,503,390 deaths across 192 countries, as of February 25, 2021[1]. An effective prophylactic vaccine remains the most effective public health measure for controlling disease spread[2]. To that end, two mRNA vaccines[3, 4] have received emergency use authorization from the FDA based on clinical efficacy of greater than 90% in the US. In addition, adenovirus-based vaccines have been approved for use in the EU, United Kingdom[5] and Russia[6], and an inactivated virus vaccine is approved in China[7]. Other candidates based on protein are currently in clinical testing[8]. With the exception of the inactivated virus vaccines[9, 10], these approved and clinical-phase candidate vaccines use only the coronavirus spike (S) protein as their immunogen.

Spike is a surface membrane-bound trimer that, by electron microscopy, gives viral particles a characteristic halo from which its family name "corona" is derived[11]. It is a type-1 viral membrane fusion protein that exists in a metastable prefusion conformation and undergoes a dramatic structural rearrangement upon engagement of the receptor binding domain (RBD) with its receptor, angiotensin-converting enzyme 2 (ACE2)[12, 13, 14], ultimately leading to membrane fusion. It has been shown that antibodies directed against the RBD can neutralize incoming virus by preventing receptor recognition and thus entry[15, 16, 17, 18, 19]. Because the RBD, as well as other regions such as the N-terminal domain (NTD) may contain neutralizing epitopes[20, 21], the full-length spike is a preferred target antigen for vaccine development. Based upon successful structure-based immunogen designs for SARS-CoV and Middle Eastern Respiratory Virus (MERS) vaccines[22, 23], mutations have been introduced to block cleavage of S into S1 and S2 subunits and stabilize a region between the central helix and heptad repeat 1, giving rise to homogeneous S protein trimers in the prefusion conformation[24]. This construct, referred to as S-2P, is the

basis for several SARS-CoV-2 vaccine candidates being delivered by adenoviral vectors[25], displayed on nanoparticles[26], or encoded by mRNA[27, 28, 29].

In contrast to vectored gene delivery vaccine platforms, adjuvanted soluble protein vaccine formulations have been approved for clinical use against several viral infections[30, 31, 32] and have a long history of being used across all age groups. Soluble protein subunit vaccines will likely require a potent adjuvant to elicit strong T and B cell responses[33]. Here we have formulated a soluble S-2P-derived protein with the well-characterized adjuvant, AS03, an oil-in-water emulsion composed of squalene, polysorbate 80, and α-tocopherol. AS03 potently induces antibodies and has been shown to increase vaccine durability, promote heterologous strain cross-reactivity[34], and to have dose-sparing effects[35, 36, 37, 38, 39]. It was licensed for use in vaccines against pandemic influenza in Europe, with approximately 90 million doses administered [35, 39, 40, 41]. Therefore, in this study, AS03-adjuvanted soluble S-2P trimers were evaluated for NHP immunogenicity and protection following SARS-CoV-2 challenge in advance of clinical trials. To date several advanced vaccine candidates have been characterized for the magnitude, quality and efficacy of the immune responses they elicit[25, 28, 42, 43]. Here we performed a thorough characterization humoral and cellular responses in the upper and lower respiratory tracts following vaccination and challenge. These studies establish that vaccine-induced antibody is sufficient for protection and highlight its role in rapid control of lower airway viral replication.

Results

Soluble spike trimers are immunogenic when adjuvanted with AS03

To create a SARS-CoV-2 protein vaccine, the S-2P stabilizing mutations were used as previously described[24]; the trimer was then expressed as a soluble protein by replacing the transmembrane domain with a T4 foldon domain, which has been shown to assist in trimerization of type-1 membrane fusion proteins[44, 45] (Fig. 1a). The resulting soluble trimeric protein immunogen is thus referred to as prefusion transmembrane-deleted spike, or preS dTM. PreS dTM trimers were then formulated by admixing with the oil-in-water emulsion, AS03. NHP were immunized intramuscularly three weeks apart with or without AS03 to confirm its role for improving antibody responses. AS03 was critical for the induction of high magnitude S-2P IgG binding and neutralization titers (Fig. S1a-b), and S-2P-specific IgA and IgG B cell responses (Fig. S1c-f). Systems serology was also performed to assess the quantitative and qualitative effector functions of vaccine responses induced by AS03. Antibodies bound to a broad array of human antibody F_C receptors and enabled F_C-mediated effector functions such as phagocytosis and complement activation (Fig. S1g,h). AS03 strongly enhanced all F_C functions equally with no skewing to a particular receptor or function. Collectively these data establish the critical role of the AS03 adjuvant for improving the magnitude and quality of antibody responses.

To study protective efficacy and perform a wider assessment of immunogenicity, rhesus macaques were immunized with 4 or 12 μg AS03-adjuvanted preS dTM; PBS was administered as a negative control (Fig. 1b). Animals did not experience any abnormal body weight or temperature changes in response to vaccination (Supplementary Table 1). Serum binding titers were detectible two weeks after the first immunization at levels that approximated those found in human convalescent donor sera (HCS) from two different benchmark cohorts; endpoint binding titers were significantly increased from $2.9x10^3$ to $7.4x10^4$ following the second immunization in the high dose group (Fig. 2a). Notably there was no significant

dose response between the 4 and 12 µg dose groups. In terms of the breadth of binding, antibody responses were observed to the S1 region and more specifically to the RBD and NTD (Fig. 2b).

Soluble spike trimers adjuvanted with AS03 induce neutralizing antibody responses

The next series of studies focused on functional antibody responses following AS03-adjuvanted preS dTM vaccination. First, the second immunization significantly improved serum avidity to S-2P in both dose groups (Fig 2c). Sera from both vaccine dose groups also showed ~100-fold higher competition with ACE2 for binding to the RBD, compared to HCS (Fig. 2d). Inhibition of viral entry was next assessed using a pseudotyped reporter virus. While neutralization was low or undetectable in most animals after the first immunization, reciprocal titers over 10^3 were achieved in nearly all animals following the boost (Fig. 2E). Similar results were seen with neutralization of live virus in a focus reduction neutralization titer assay, and these responses were generally 10-fold higher than those of HCS (Fig. 2F). Based on recent outbreaks of variant strains, we assessed neutralization against the B.1.1.7 "UK" and B.1.351 "South African" variants. Notably, there was ~2-fold decrease against the B.1.1.7 variant, and ~5 to 10 - fold reduction against the B.1.351 variant (Fig. S2).

Soluble spike trimers adjuvanted with AS03 induce a mixed CD4 T cell response

Since adjuvants also have an important effect on the magnitude and quality of CD4 T cells, we measured the frequency of spike specific memory T_H1 (IL-2, TNF, and IFNγ), T_H2 (IL-4, IL-13), Th17 (IL-17) and T_{FH} ($CXCR5^+$, $PD\text{-}1^+$, $ICOS^+$) IL-21 and CD40 ligand responses from PBMCs by multi-parameter flow cytometry. Two weeks following the boost (week 5), both T_H1 and T_H2 cytokines were detected (Fig. 3a). In assessing individual cytokines, the T_H1 response was comprised mostly of IL-2 and TNF with minimal IFNγ production, indicative of a "T_H0" phenotype[46, 47] (Fig. 3b). Of note, antigen-specific IL-21 production and CD40 ligand expression were detected in both CD4 memory and T_{FH}-gated PMBC subsets, supporting their role in the robust antibody responses induced following vaccination (Fig. 3c). To

161 further analyze cytokine production on a single cell-basis, Boolean gating was used to show the various
162 combinations of cytokines (Fig. 3D). Greater than ~89% were CD40L+, a sensitive marker for antigen
163 specific cells. Notably, just 6.5% of cells produced only T_H2 cytokines, while ~27% produced
164 combinations of IL-2 or TNF, and IL-4 or IL-13, characterized as a mixed or "T_H0" phenotype. CD8 T
165 cell responses were largely undetectable (Fig. 3e).
166
167 Soluble spike trimers adjuvanted with AS03 protect NHP from high dose SARS-CoV-2 challenge
168 Prior NHP vaccine studies[25, 48] have used varying doses of the USA-WA1/2020 isolate ranging from 10^4
169 to 10^6 PFU for nasal and intratracheal challenge. In addition, passaging of the USA-WA1/2020 isolate has
170 led to mutations in the furin cleavage site that can limit pathogenicity and results in variation of the
171 amount and duration of infection in NHP. Thus, in this study, NHP were challenged 3 weeks following
172 the boost with a new sequence-validated stock of the USA-WA1/2020 isolate that was administered at a
173 high dose of $3x10^6$ PFU SARS-CoV-2 given intranasally and intratracheally. Lower airway protection
174 was assessed using subgenomic RNA (sgRNA), as a quantitative metric of replicating virus[49] in BAL
175 (Fig. 4a). At day 2, 6/7 (86%) PBS control animals had detectable sgRNA, compared to 6/8 (75%) and
176 3/8 (38%) in the 4 µg and 12 µg dose groups, respectively. By day 4, 5/7 (71%) of PBS control animals
177 were positive, but sgRNA was significantly reduced to 2/8 (25%) or 0/8 (0%) in the 4 µg and 12 µg
178 vaccine dose groups, respectively. By day 7, sgRNA was detectable in 4/7 (57%) PBS controls but only
179 1/16 (6%) vaccinated animals. To assess upper airway protection, sgRNA was quantified in nasal swab
180 extracts (Fig. 4b). Both vaccine groups showed significant sgRNA reduction of ~1-3 Log_{10} on day 2. By
181 day 4, 5/7 (71%) PBS controls had detectible sgRNA (10^4), while only 2/8 (25%) and 0/8 (0%)
182 vaccinated NHP had detectable sgRNA in the 4 µg and 12 µg dose groups, respectively. Thus, AS03-
183 adjuvanted preS dTM provided significant protection in the upper and lower airways from this robust
184 SARS-CoV-2 challenge.
185

To further substantiate the vaccine protection, lung tissue was analyzed for viral antigen, inflammation, and eosinophil infiltration in half of the animals in each group 7 days following challenge (Fig. 4c-e). Viral antigen was detected in at least 1 lobe of 3/4 PBS control animals, while antigen was undetectable in the high-dose vaccinated animals and had only limited detection in 2 of the low-dose vaccinated animals. Vaccination at either dose trended to reduce both tissue inflammation (Fig. 4d) and the presence of eosinophils (Fig. 4f), though these observations did not reach statistical significance.

SARS-CoV-2 challenge boosts antibody titers in the lung

To further investigate how T cells or antibodies may have influenced protection in the respiratory tissues, we assessed T cell responses in the BAL and PBMC and antibody responses in the serum, BAL and nasal washes at various time points post challenge. Compared to the peak T cell responses after the second immunization at week 5 (restimulated with S peptides, Fig. 3a,b) memory PBMC CD4 and CD8 T cell responses were largely unchanged 7 to 14 days post challenge (Fig. S3a,b). However in BAL samples, spike-specific IL-2, IFNγ, and IL-13 recall responses were increased in the vaccinated groups compared to week 5, but not in the PBS controls (Fig. S3c,d). To assess the primary T cell response to infection, cells were restimulated with peptides to nucleoprotein, which is not present in the vaccine. Here we noted that the SARS-CoV-2 challenge induced a strong T_H1 response in the BAL but not in PBMCs by day 14 that was specific to the PBS control animals (Fig. S3e,f). These data suggest that vaccine-elicited immune responses controlled the infection before a detectable primary T cell response could be generated in BAL or PBMCs.

Because vaccinated animals showed no detectable primary N-specific T cell response to the challenge in BAL or PBMCs, it suggested rapid control of infection by the vaccine in the airways, which we hypothesized might be mediated by antibodies. To assess this, we performed a kinetic analysis of antibody responses in BAL and nasal washes up to two weeks post challenge. Remarkably, S-2P IgG binding titers were significantly increased in the BAL from vaccinated animals just 2 days post challenge

and remained higher than the control animals through day 7 (Fig. 5a). In contrast, IgA and IgG responses to the challenge developed only by day 14 in the PBS control animals consistent with the kinetics of a primary response (Fig. 5a,b). Notably this anamnestic response in the vaccinated animals was specific to the BAL, as there was no increase in S-2P IgG titers in the nasal wash (Fig. 5c) or the serum (Fig. 5d) post challenge. Importantly, the primary antibody response was evident in blood and upper and lower airways by day 14 in the PBS control animals. Based on the rapid anamnestic response in BAL in the vaccine groups, we next determined whether this was specific to S-2P antibodies, or if the challenge was causing a general increase in IgG. Indeed, there was an increase in total IgG in BAL of vaccinated animals at 2 days post challenge, continuing through day 4 and decreasing by day 7, while PBS control animals had a smaller increase on day 4 only (Fig. S4a). We next assessed whether other antibody specificities were increased in BAL post challenge. Because all NHP used in our studies have had earlier vaccination against measles, we assessed measles antibody titers in BAL. Consistent with increases in spike and total IgG titers in BAL, vaccinated animals similarly showed a significant increase in measles antibodies on days 2 and 4 compared to pre-challenge, while several PBS control animals also increased on day 4 (Fig. S4b). Finally, to assess whether this increase in total IgG could be due to increased general transudation into the lung from the serum, we assessed the serum protein albumin levels in BAL. Albumin levels in BAL were not significantly increased in the vaccinated or PBS control animals following SARS-CoV-2 challenge (Fig. S4c). These data show that SARS-CoV-2 challenge leads to a rapid and transient local increase in IgG that occurs earlier in vaccinated animals.

Vaccine induced IgG is sufficient to confer protection from SARS-CoV-2 challenge

Based on the high antibody and neutralizing titers in the blood and rapid anamnestic antibody responses in the BAL following challenge, we hypothesized that IgG was mediating protection. To directly assess whether vaccine induced antibody was sufficient to mediate protection, NHP IgG was purified from pooled plasma three weeks following the second vaccination just prior to the challenge and passively transferred to hamsters (Fig. 6a). A total of 10 mg or 2 mg total IgG per animal from AS03-adjvuanted

preS dTM vaccinated NHP or from animals prior to vaccination as a negative control was administered to 8 individual hamsters per group. This resulted in approximately 125 mg and 25 mg IgG/kg bodyweight for the 10 and 2 mg dose groups, respectively (Fig. S5a). PBS was administered to an additional group as a negative control, and the highly potent and clinically approved SARS-CoV-2 mAb, LY-CoV555[50] was administered to another group at 10 mg/kg as a positive control. Just prior to challenge, serum S-2P titers were confirmed in all but 2 animals, which were subsequently excluded (Fig. S5 b,c). Notably, the LY-CoV555 mAb recipient animals had higher ELISA binding titers than those that received polyclonal post-vaccination IgG. Hamsters that received only PBS prior to SARS-CoV-2 challenge lost an average of 10-15% of their bodyweight at day 6, a primary outcome measure of disease progression (Fig. 6b, Supplementary Table 2). Hamsters that received 10 mg of post-vaccination IgG had little weight loss and gained weight at a rate almost equivalent to that of the LY-CoV555 recipient hamsters. This protection was dose-dependent, as the animals that received 2 mg of post-vaccination IgG showed weight loss of ~7% by day 6. Finally, individual animal serum S-2P binding titers were strongly correlated with body weight change, confirming the effect of IgG in protection from challenge (Fig. 6c). Taken together, these data show that the AS03-adjuvanted preS dTM vaccine elicited IgG sufficient to mediate protection *in vivo* against SARS-CoV-2 infection.

Discussion

In this study, an AS03-adjuvanted soluble prefusion S protein vaccine formulation produced by Sanofi Pasteur and GlaxoSmithKline was evaluated for its ability to protect nonhuman primates against SARS-CoV-2 challenge in advance of clinical trials. Although SARS-CoV-2 mRNA- and adenovirus-based vaccine candidates have been authorized for emergency use in various countries, adjuvanted protein vaccines provide an additional vaccine platform to prevent disease that could be broadly useful in all age groups based on their long history and safety record with other viral infections. A key aspect of these studies was to provide new insights into the mechanisms of protection, most notably in the lung, which is critical for understanding how vaccines limit disease, a primary endpoint in all clinical trials.

By comparing the immune response to preS dTM formulations with and without AS03, it is clear that AS03 is critical for the induction of protective antibody responses, as has been previously observed with influenza[35, 36, 51, 52] and respiratory syncytial virus (RSV)[53]. The CD4 responses to spike were primarily T_H0 given the relative limited IFNγ production[46] and T_H2. In mouse studies, IL-4 and IL-13 production was also observed following vaccination with an inactivated influenza/AS03 formuation[54]. Previous human studies of AS03 with hepatitis B surface antigen[55] and influenza hemagglutinin[56] have observed strong IL-2 and TNF production with lower IFNγ responses. However, IFNγ responses were recently documented in humans with AS03 and a similar antigen (SCB-2019)[57], suggesting that the CD4 profile might differ depending on the species and the antigen. Based on mouse and other animal models, vaccine-induced T_H2 responses have been proposed to contribute to enhanced respiratory disease (ERD)[58, 59, 60] as was observed in children given inactivated measles[61] and RSV[62] vaccines. Similarly, SARS vaccines formulated with the T_H2-skewing adjuvant, alum, have been reported to induce immunopathology following challenge in mice, including eosinophilia[63]. Other studies suggest ERD is driven by nonfunctional and poorly matured antibodies[58, 64, 65]. Regardless of the mechanism, and in contrast to those findings, following SARS-CoV-2 challenge there was limited evidence of viral infection and there

was a trend toward lower inflammation and eosinophil infiltration in lung tissue from vaccinated animals compared to PBS controls, indicating no enhanced disease.

A major focus of this study was to fully characterize the magnitude, quality and location of antibody responses. The NHP model has been used extensively for COVID-19 vaccine development and shares characteristics of mild human disease. Thus, a major advantage of using NHP is the ability to analyze immune responses in the mucosa of the upper and lower airways. Regarding the magnitude of antibody responses, pseudo- and live virus- neutralization titers were above 10^3 in most animals 2 weeks after the second immunization of AS03-adjuvanted preS dTM. These responses are comparable to prior studies using similar assays following 100 µg of the mRNA nanoparticle vaccines, mRNA1273[28] and BNT162b2[48] and importantly are superior to those from convalescent humans.

The AS03-adjvuanted preS dTM was able to rapidly reduce viral replication in both the upper and lower airways (BAL) by day 2, with no detectable virus in any of the animals in the high dose group by day 4. Comparing these results to other vaccines is difficult based on differences in the challenge stock dose and virulence. Here we have used a high challenge dose of $3x10^6$ PFU, which is 5-200 fold higher than the doses used to evaluate mRNA1273[28], Ad26.COV2-S[25], ChAdOx1 nCoV-19[43], and NVX-CoV2373[42], but similar to that used for BNT162b2[48]. The relatively higher challenge dose used here may in part explain why there was not complete reduction in viral titers at day 2, as was observed with other vaccines tested in NHP using lower challenge doses. Similarly we observed nasal swab titers of ~$2x10^6$ sgRNA copies/mL in the control animals at day 2, 10-50 fold higher than previously reported in other NHP studies by us and others[28, 43], likely reflecting both the more virulent challenge and improved sgRNA extraction methods.

Because significant protection was conferred by vaccination with AS03-adjuvanted preS dTM, it was critical to investigate the potential mechanisms for this effect. Consistent with data from most protein

306 subunit vaccine studies in humans with AS03 and other adjuvants, CD8 T cell responses were
307 undetectable. These data suggest they would have a limited role in primary, rapid protection in this
308 model. By contrast, potent antigen-specific CD4 T cells were comprised of Th0, T_H2 and T_{FH} cytokines
309 and expressed CD40L, which are optimal for generating robust antibody responses. In terms of having
310 effector functions to mediate protection, a direct protective role of CD4 T cells would have required cell
311 depletion prior to challenge and was not assessed in this study.
312
313 Based on the early control of infection seen by day 2, it is likely that antibodies had a significant role in
314 neutralizing replicating virus. That neutralizing antibodies could protect against challenge has been shown
315 in correlative analyses with other SARS-CoV-2 vaccine candidates[28, 66]. Moreover, prior studies have
316 shown a protective effect from passively transferred convalescent sera to hamsters[67] and NHP[68].
317 However, here is the first demonstration that vaccine-elicited IgG could protect against challenge,
318 providing direct evidence that antibodies are sufficient to mediate protection. An additional finding that
319 substantiates a role for antibodies was the rapid increase in IgG responses in the lung as early as 2 days
320 following challenge in NHP. Mucosal antibody responses to vaccination have been well documented,
321 including in response to polio[69, 70, 71], influenza[72, 73] and RSV[74, 75] vaccines. Moreover, neutralizing BAL
322 responses have been observed in humans in the initial days after symptom onset[76]. However, to the best of
323 our knowledge, this is the first report of vaccine-directed anamnestic lung responses to challenge. This
324 rapid increase in spike IgG appears specific to the BAL compartment and was not observed in the upper
325 airway or serum post-challenge. A notable finding was that there was also a transient increase in total IgG
326 titers and measles antibody from prior vaccination in the BAL at day 2, yet albumin levels were not
327 increased. These data suggest that the increase in antibodies may not be due to a general transudation of
328 proteins from increased vascular leakage or bulk vesicular transport. We speculate that this increase in
329 total and antigen-specific IgG could occur through a general activation of memory B cells in the lung,
330 perhaps directly from TLR-sensing of viral RNA[77] or through bystander activation from activated S-
331 specific CD4 T cells. Together this could explain why IgG titers were higher in vaccinated animals on day

2, while PBS controls showed a smaller increase in total and measles IgG only on day 4. While antibody secreting cell (ASC) enumeration was not possible in this study, future studies will examine changes in lung resident ASCs and investigate whether an increase in BAL antibodies is specific to this vaccine or is generalizable to other vaccine platforms. Nevertheless, these data highlight the potential role of ASCs in contributing to control of viral infections in the lung.

In conclusion, this report highlights that potent serum antibody responses are induced by soluble S trimers formulated with the oil-in-water emulsion adjuvant AS03, which conferred protection in the upper and lower airways following SARS-CoV-2 challenge. This vaccine induced IgG responses sufficient to protect from SARS-CoV-2 challenge, and the rapid anamnestic response in the lower airway likely contributed to protection at this site. These data support the clinical development of the AS03-adjuvanted preS dTM vaccine for limiting SARS-CoV-2 infection and protecting against COVID-19 morbidity and mortality.

Materials and Methods

Immunogen

The SARS-CoV-2 recombinant vaccine candidate consists of purified recombinant prefusion spike (S) protein (SARS-CoV-2 prefusion-stabilized S delta TM (preS dTM)) adjuvanted with AS03.

The preS dTM was produced from a Sanofi Pasteur proprietary cell culture technology based on the insect cell – baculovirus system, referred to as the Baculovirus Expression Vector System (BEVS). The preS dTM sequence was designed based on the Wuhan YP_009724390.1 strain S sequence, but modified to improve the conformation, stability, trimerization and facilitate the purification. The modifications comprise mutation of the S1/S2 furin cleavage site, introduction of two proline mutations in the C-terminal region of S2 domain, deletion of the transmembrane and cytoplasmic region and replacement by the T4-foldon trimerization domain[24]. Briefly, the modified sequence was cloned into a baculovirus transfer plasmid, which was then used to generate a recombinant baculovirus containing the gene of interest. The recombinant baculovirus was first amplified in expreSF+ insect cells prior to infecting a large scale expreSF+ insect cells culture in suspension. After incubation, the recombinant protein was purified from the supernatant using several affinity and chromatography columns. Based on an ACE2 binding assay, the preS dTM used in the study were quantified at 4 µg and 12 µg for a total protein content of 5 and 15 µg, for the low and high doses respectively.

Adjuvant and formulation

AS03 is an Adjuvant System composed of α-tocopherol, squalene and polysorbate 80 in an oil-in-water emulsion[78]. Vaccine doses were formulated by diluting the appropriate dose of preS dTM with PBS-tween to 250 µL, then mixing with 250 µL AS03, followed by inversion five times for a final volume of 500 µL. Each dose of AS03 contains 11.86 mg α-tocopherol, 10.69 mg squalene and 4.86 mg polysorbate-80 (Tween 80) in PBS.

370

371 *Animals, immunizations, challenges and sampling*

372 Rhesus macaques were randomized into groups of 8 based on age and body weight; each group had 2
373 females and 6 males, except for the PBS control group, which only had 5 males. All animals had a history
374 of measles vaccination. SARS-CoV-2 vaccine formulations were administered by intramuscular injection
375 into the right deltoid for both immunizations, three weeks apart. Whole blood was collected weekly into
376 EDTA-containing tubes and also 1, 4 and 7 days after each immunization for complete blood
377 count/chemistry profiling. PBMC and plasma were then collected from whole blood following ficoll
378 purification. For SARS-CoV-2 challenge, virus was obtained from Operation Warp Speed: strain- 2019-
379 nCoV/USA-WA1/2020, Lot# 70038893; BEI resources catalog no. NR-53780. Virus was inoculated
380 intranasally (0.5 mL per nostril) and intratracheally (3 mL) for a total of $3x10^6$ PFU per animal.
381 Bronchiolar/alveolar lavage (BAL) sampling was performed 5 weeks after vaccination and 2, 4 and 7
382 days after challenge. Nasal swabs for sgRNA PCR were taken 5 weeks after vaccination and 2, 4 and 7
383 days after challenge; nasal washes (~5 mL PBS) were collected at weeks 0 and 5, and 1, 2, 4, 7 and 14
384 days post challenge. Half the animals in each group were necropsied at day 7 and 14 post challenge,
385 where lung tissue was collected for histopathology.

386

387 In a separate study, 4 groups of 6 rhesus macaques were similarly vaccinated, but with lower doses of 1.3
388 and 3.9 µg preS dTM + AS03, or 3.9 µg preS dTM without AS03, or PBS alone. Animals were then
389 boosted at week 3 with 2 and 6.1 µg preS dTM + AS03, or 6.1 µg preS dTM without AS03, or PBS alone.
390 Immunogenicity data from this study are found in Figure S2. IgG were purified from animals given 3 µg
391 preS dTM + AS03 either before immunization or 3 weeks following the second immunization for use in
392 passive transfer to hamsters, Figure 6.

393

394 For passive transfer studies, 6–8-week-old Golden Syrian hamsters were randomized into groups of 8
395 based on weight, each group having 4 males and 4 females. IgG was passively transferred by

intraperitoneal injection 1 day prior to challenge. SARS-CoV-2 challenge virus (strain- 2019-nCoV/USA-WA1/2020, Lot# 70038893; BEI resources catalog no. NR-53780) was introduced intranasally at a dose of $3x10^4$ PFU administered in a final volume of 100 µL and split between each nostril. Body weight and clinical observations were made daily; serum was sampled just prior to challenge; oral swabs were taken 0, 2, 4, 7 and 10 days post challenge for viral load determination.

Ethics statement

Macaques were housed at the NIH (for immunizations) and Bioqual, Inc. (for challenge); hamsters were housed at Bioqual, Inc. All animals were cared for in accordance with American Association for Accreditation of Laboratory Animal Care standards in accredited facilities. All animal procedures were performed according to protocols approved by the Institutional Animal Care and Use Committees of the National Institute of Allergy and Infectious Diseases, National Institutes of Health and Bioqual, Inc. NHP studies were performed under NIH animal study protocol #VRC-20-870; hamster studies were performed under animal study protocol #VRC-20-872.

Human convalescent sera

Two panels of samples from human patients who had recovered from SARS-CoV-2 disease were used in parallel. The first panel referred to as "NIH" has been described previously[28]. Additionally, an 18-sample panel collected by Operation Warp Speed and distributed by Battelle and BEI Resources was also used, referred to here as "OWS". Informed consent was obtained from all participants. Participants had a history of laboratory-confirmed SARS-CoV-2 infection before they provided serum.

Serology

Antibody titers to various SARS-CoV-2 derived antigens were assayed as previously described[28]. Briefly, endpoint binding titers were measured by standard sandwich ELISA using proline-stabilized spike protein (S-2P). Binding to SARS-CoV-2 S1, receptor-binding domain (RBD), and N-terminal domain (NTD)

spike subdomains was performed using Mesoscale Discovery ELISA[28], using biotinylated subdomain proteins prepared as described previously[79].

Total IgG antibody titers were quantitated by using the Human IgG ELISA ^{BASIC} kit (ALP) (Mabtech) following manufactures directions. Samples were read by MSD plate reader (Sector Imager 600). Antibody titers to measles were quantitated by using Monkey Anti-Measles IgG ELISA kit (Alpha Diagnostics International) following manufactures directions. The optical density (OD) of each well was read at 450 nm by SpectraMax Paradigm Multi-Mode Microplate Reader (Molecular Devices). Albumin levels were measured by bead-based single-plex assay using Luminex. The albumin analyte was selected and measured using MILLIPLEX MAP Human Kidney Injury Magnetic Bead Panel 2 (Millipore Sigma) following manufacturer's instructions. Fluorescence data were collected on MAGPIX with Bio-Plex ManagerTM MP software (BioRad).

ACE2 binding inhibition was also performed via Mesoscale Discovery 384-well, 4-Spot Custom Serology SECTOR plates precoated with RBD; plasma was applied at a starting dilution of 1:10 followed by 10-fold serial dilutions. Binding was detected with SULFO-TAG–labeled ACE2 (Meso Scale Diagnostics).

For avidity analyses, plasma samples were heated at 56 °C for 45 min to complement-inactivate and reduce potential risk from any residual virus and immediately used or stored at -80°C for later use. 96-well plates (Nunc MaxisorpTM, Thermo Fisher) were coated with 100 µL of 1 µg/mL SARS-CoV-2 S-2P in 1x PBS for 16 hrs at 4°C. Plates were washed 3x in washing buffer (1x PBS, 0.2% Tween20, pH 7.4) using a Biotek 405 Microplate Washer and blocked with 200 µL blocking buffer (1 x PBS-T: 0.14 M NaCl, 0.0027 M KCl, 0.05% Tween 20, 0.010 M PO43-, pH 7.4) for 2 hrs at RT and washed 3x. Plasma/serum samples were serially diluted (starting dilution 1:100 and 4-fold dilutions) in blocking buffer and 100 µL was transferred to the plates. After 1 hour of incubation, plates were washed, and half of the samples were then incubated with 100 µL 1x PBS while the other half of the paired samples were

448 treated with 100 µL 1.0 M sodium thiocyanate solution (NaSCN, Sigma-Aldrich) for 15 minutes at room
449 temperature (RT) and washed 6x. Plates were incubated for 1 hr with 100 µL of goat-anti-human IgG
450 (H+L, Cat#PA1-8463) or goat-anti-monkey IgG (H+L, Cat#A18811) secondary antibody conjugated to
451 horseradish peroxidase (HRP, Thermo Fisher) in blocking buffer at 1:10,000 or 1:4,000 dilution,
452 respectively. Plates were washed 3x and developed by addition of 100 µL KPL SureBlueTM TMB
453 Microwell Peroxidase Substrate (1-Component, SeraCare, Cat#52-00-01) for 10 min. The reaction was
454 quenched by addition of 100 µL 1 N H2SO4 and absorbance was measured at a test wavelength of 450
455 nm and reference wavelength of 650 nm using SoftMax Pro software version 6.5 on a Spectramax
456 Paradigm Microplate reader (Molecular Devices). The avidity index (AI) was calculated using the ratio of
457 the NaSCN-treated serum dilution giving an OD of 0.5 to the PBS-treated serum dilution giving an OD of
458 0.5 after 5PL curve-fitting in Graphad Prism. Reported AI is the average of two independent experiments,
459 each containing duplicate samples. Samples with an OD < 0.5 could not be interpolated and were
460 excluded from analysis.
461
462 To produce SARS-CoV-2 pseudotyped lentivirus, a codon-optimized CMV/R-SARS-CoV-2 S (Wuhan-1,
463 GenBank: MN908947.3) plasmid was constructed and subsequently modified via site-directed
464 mutagenesis to contain the D614G mutation. Further mutations were integrated into the D614G
465 background to recapitulate the spike mutations of both the B.1.1.7 (UK) and B.1.351 (RSA) variants.
466 Pseudoviruses were produced by co-transfecting HEK293T/17 cells (ATCC CRL-11268) with plasmids
467 encoding a luciferase reporter, a lentivirus backbone, and the SARS-CoV-2 S genes into HEK293T/17
468 cells (ATCC CRL-11268) as previously described[80]. A human transmembrane protease serine 2
469 (TMPRSS2) plasmid was co-transfected to produce pseudovirus[81]. Neutralizing antibody responses in
470 sera were assessed by pseudoneutralization assay as previously described[3, 22]. Briefly, heat-inactivated
471 sera were serially diluted in duplicate, mixed with pseudovirus previously titrated to yield 10^4 RLU, and
472 incubated at 37°C and 5% CO2 for roughly 45 minutes. 293T-hACE2.mF cells were diluted to a
473 concentration of 7.5 x 10^4 cells/mL in DMEM (Gibco) supplemented with 10% Fetal Bovine Serum

(FBS) and 1% Penicillin/Streptomycin and added to the sera-pseudovirus mixture. Seventy-two hours later, cells were lysed and luciferase activity (in relative light units (RLU)) was measured using a SpectraMaxL (Molecular Devices) luminometer. Percent neutralization was normalized, considering uninfected cells as 100% neutralization and cells infected with pseudovirus alone as 0% neutralization. ID_{50} titers were determined using a log(agonist) vs. normalized-response (variable slope) nonlinear regression model in Prism v8 (GraphPad).

For neutralization of authentic SARS-CoV-2 virus, a focus reduction neutralization titer (FRNT) assay was performed as previously described[82]. Plasma/serum were serially diluted (three-fold) in serum-free Dulbecco's modified Eagle's medium (DMEM) in duplicate wells and incubated with 100–200 FFU infectious clone derived SARS-CoV-2-mNG virus[83] at 37 °C for 1 h. The antibody-virus mixture was added to VeroE6 cell (C1008, ATCC, #CRL-1586) monolayers seeded in 96-well blackout plates and incubated at 37 °C for 1 h. Post-incubation, the inoculum was removed and replaced with pre-warmed complete DMEM containing 0.85% methylcellulose. Plates were incubated at 37 °C for 24 h. After 24 h, methylcellulose overlay was removed, cells were washed twice with PBS and fixed with 2% paraformaldehyde in PBS for 30 min. at room temperature. Following fixation, plates were washed twice with PBS and foci were visualized on a fluorescence ELISPOT reader (CTL ImmunoSpot S6 Universal Analyzer) and enumerated using Viridot[84]. The neutralization titers were calculated as follows: 1 - (ratio of the mean number of foci in the presence of sera and foci at the highest dilution of respective sera sample). Each specimen was tested in two independent assays performed at different times. The FRNT-mNG_{50} titers were interpolated using a 4-parameter nonlinear regression in GraphPad Prism 8.4.3. Samples with an FRNT-mNG_{50} value that was below the limit of detection were plotted at 10. For these samples, this value was used in fold reduction calculations.

Quantification of antigen-specific B cells

Cryopreserved PBMC were stained for antigen-specific B cells and subsets (Figure S6) using the following panel: IgM BUV395 (clone G20-127, Becton Dickenson), CD8 BUV665 (clone RPAT8, BD), CD56 BUV737 (clone NCAM16, BD), IgD FITC (Southern Biotech), IgA Dy405 (polyclonal, Jackson Immunoresearch), aqua LIVE/DEAD (Invitrogen), CD14 BV785 (clone M5E2, BioLegend), CD20 Alexa700-PE (clone 2H7, vaccine research center), IgG Alexa700 (clone G18-145, BD), CD3 Cy7APC (clone SP34-2, BD Pharmingen). Biotinylated prefusion-stabilized spike (S-2P) and spike subdomain (NTD, RBD) probes were produced as previously described[79] and conjugated to streptavidin-labeled dyes (BD) to yield the following and streptavidin-conjugated B cell probes, NTD SA-BB700 (BD), RBD SA-BV650 (BD), and S-2P SA-APC (BD). PBMC were thawed into cRPMI + 10% FBS[85], washed with PBS, and stained with aqua LIVE/DEAD kit in PBS for 20 min. at 4 °C. Staining was then completed with the remainder of the antibody and probe cocktail described above for 45 min. at 4 °C, and washed twice with PBS before flow cytometry.

Intracellular Cytokine Staining

To measure vaccine-specific T cell responses, cryopreserved PBMC were thawed and rested overnight in a 37C/5% CO2 incubator. The next morning, cells were stimulated with SARS-CoV-2 spike protein (S1 peptide pools, JPT Peptide Technologies, Inc.) at a final concentration of 2 μg/ml in the presence of monensin and costimulatory antibodies anti-CD28 and -49d (clones CD28.2 and 9F10, BD Biosciences) for 6 hours. Negative controls received an equal concentration of DMSO (instead of peptides) and co-stimulatory antibodies. Intracellular cytokine staining and gating for CD4, CD8 was performed as previously described[86] except the following monoclonal antibodies were added: PD-1 BUV737 (clone EH12.1, BD Biosciences) in place of PD-1 BV785, TNF-FITC (clone Mab11, BD Biosciences) in place of IL-5 BB515, and CD154 (CD40L) BV785 (clone 24-31, BioLegend). T_{FH} subsets were gated as $CXCR5^+$, $PD\text{-}1^+$, $ICOS^+$. Aqua LIVE/DEAD kit (Invitrogen) was used to exclude dead cells. All antibodies were previously titrated to determine the optimal concentration.

524

525 *Flow cytometry*

526 All phenotyping and ICS data were acquired on an BD FACSymphony flow cytometer and analyzed
527 using FlowJo version 9.9.6 (Treestar, Inc., Ashland, OR).

528

529 *Luminex Isotype and FcR Binding Assay*

530 To determine relative concentrations of antigen-specific antibody isotypes and Fc-receptor binding
531 activity in the rhesus samples, a customized Luminex isotype assay was performed as previously
532 described[87]. Antigens including SARS-CoV-2 full length spike (Eric Fischer, DFCI) and RBD (kindly
533 provided by Aaron Schmidt, Ragon Institute) were covalently coupled to Luminex microplex
534 carboxylated bead regions (Luminex Corporation) using NHS-ester linkages with Sulfo-NHS and EDC
535 (Thermo Fisher Scientific) according to manufacturer recommendations. Immune complexes were formed
536 by incubating antigen-coupled beads with diluted samples while rotating overnight. Mouse-anti-rhesus
537 antibody detectors were then added for each antibody isotype (IgG1, IgG2, IgG3, IgG4, IgA, NIH
538 Nonhuman Primate Reagent Resource supported by AI126683 and OD010976). Then, tertiary anti-
539 mouse-IgG detector antibodies conjugated to PE were added. Flow cytometry was performed using a an
540 iQue Plus Screener (Intellicyt) with a robot arm (PAA). Analysis of the flow cytometry data was
541 performed using iQue Intellicyt software.

542

543 *Systems serology*

544 In order to quantify antibody functionality of plasma samples, bead-based assays were used to measure
545 antibody-dependent cellular phagocytosis (ADCP), antibody-dependent neutrophil phagocytosis (ADNP)
546 and antibody-dependent complement deposition (ADCD), as previously described[88, 89, 90]. SARS-CoV-2
547 spike protein (kindly provided by Eric Fischer, DFCI) was coupled to fluorescent streptavidin beads
548 (Thermo Fisher) and incubated with diluted plasma samples to allow antibody binding to occur. For
549 ADCP, cultured human monocytes (THP-1 cell line, ATCC) were incubated with immune complexes to

induce phagocytosis. For ADNP, primary PMBCs were isolated from whole blood from healthy donors using an ammonium-chloride-potassium (ACK) lysis buffer. After phagocytosis of immune complexes, neutrophils were stained with an anti-CD66b Pacific Blue detection antibody (Biolegend). For detection of complement deposition, lyophilized guinea pig complement (Cedarlane) was reconstituted according to manufacturer's instructions and diluted in a gelatin veronal buffer with calcium and magnesium (Boston BioProducts). After antibody-dependent complement deposition occurred, C3 bound to immune complexes was detected with FITC-Conjugated Goat IgG Fraction to Guinea Pig Complement C3 (MP Biomedicals).

For quantification of antibody-dependent NK cell activation[91], diluted plasma samples were incubated in Nunc MaxiSorp plates (Thermo Fisher Scientific) coated with antigen. Human NK cells were isolated the evening before using RosetteSep Human NK cell Enrichment cocktail (STEMCELL Technologies) from healthy buffy coat donors and incubated overnight with human recombinant Interleukin 15 (IL-15) (STEMCELL Technologies). NK cells were incubated with immune complexes, CD107a PE-Cy5 (BD), Golgi stop (BD) and Brefeldin A (BFA, Sigma-Aldrich). After incubation, cells were stained using anti-CD16 APC-Cy7 (BD), anti-CD56 PE-Cy7 (BD) and anti-CD3 Pacific Blue (BD), and then fixed (Perm A, Life Tech). Intracellular staining occurred with anti-IFNγ FITC (BD) and anti-MIP-1β PE (BD) after permeabilizing the NK cells with Perm B (Thermo Fisher). Flow cytometry acquisition of all assays was performed using the iQue Screener Plus (Intellicyt) and an S-LAB robot (PAA). For ADCP, phagocytosis events were gated on bead-positive cells. For ADNP, neutrophils were identified by gating on CD66b+ cells, phagocytosis was identified by gating on bead-positive cells. A phagocytosis score for ADCP and ADNP was calculated as (percentage of bead-positive cells) x (MFI of bead-positive cells) divided by 10,000. ADCD quantification was reported as MFI of FITC-anti-C3. For antibody-dependent NK activation, NK cells were identified by gating on CD3-, CD16+ and CD56+ cells. Data were reported as the percentage of cells positive for CD107a, IFNγ, and MIP-1β.

Quantification of subgenomic RNA following challenge

Nasal swabs and bronchoalveolar-lavage (BAL) fluid were collected 2, 4, and 7 days post-challenge. At the time of collection, nasal swabs were frozen in 1mL of PBS containing 1 µL of SUPERase-In RNase Inhibitor (Invitrogen) and frozen at -80 °C until extraction. Nasal specimens were thawed at 55 °C, and the swab removed. The remaining PBS was mixed with 2 mL of RNAzol BD (Molecular Research Center) and 20 µL acetic acid. At the time of collection, 1 mL of BAL fluid was mixed with 1 mL of RNAzol BD containing 10 µL acetic acid and frozen at -80 °C until extraction. BAL specimens were thawed at room temperature and mixed with an additional 1 mL of RNAzol BD containing 10 µL acetic acid.

Total RNA was extracted from nasal specimens and BAL fluid using RNAzol BD Column Kits (Molecular Research Center) and eluted in 65 µL H_20. Subgenomic SARS-CoV-2 E (envelope) mRNA was quantified via polymerase chain reaction (PCR) using a technique similar to that described previously[1]. Reactions were conducted with 5 µL RNA and TaqMan Fast Virus 1-Step Master Mix (Applied Biosystems) with 500 nM primers and 200 nM probes. Primers and probes were as follows:

sgLeadSARSCoV2_F: 5'-CGATCTCTTGTAGATCTGTTCTC-3'

E_Sarbeco_P: 5'-FAM-ACACTAGCCATCCTTACTGCGCTTCG-BHQ1-3'

E_Sarbeco_R: 5'-ATATTGCAGCAGTACGCACACA-3'

Reactions were run on a QuantStudio 6 Pro Real-Time PCR System (Applied Biosystems) at the following conditions: 50 °C for 5 min, 95 °C for 20 sec, and 40 cycles of 95 °C for 15 sec and 60 °C for 1 min. Absolute quantification was performed in comparison to a standard curve. For the standard curve, the E subgenomic mRNA sequence was inserted into a pcDNA3.1 vector (Genscript) and transcribed

using MEGAscript T7 Transcription Kit (Invitrogen) followed by MEGAclear Transcription Clean-Up Kit (Invitrogen). The lower limit of quantification was 50 copies.

Histopathology

Histopathological analyses were performed as described previously[28]. Immunohistochemistry was used to visualize SARS-CoV-2 nucleocapsid antigen (rabbit polyclonal, GeneTex), and eosinophils by staining for eosinophil peroxidase (rabbit polyclonal, Atlas Antibodies). Inflammation was scored on the following scale based on % tissue affected: **0**, 0%; **1**, <10%; **2**, 10-25%; **3**, 26-50%; **4**, >50%. Viral antigen from IHC was scored on the following scale: **0**, minimal to absent; **1**, minimally abundant but clearly present; **2**, mildly abundant; **3**, moderately abundant; **4**, abundant. Eosinophils from IHC were scored on the following scale: **0**, within normal limits; **1**, minimal increase; **2**, mild increase; **3**, moderate increase; **4**, abundant.

Statistics

All statistical analyses were performed in Prism (version 8.4, GraphPad). For comparisons between NHP vaccine groups at a single time point or dilution, a Kruskal-Wallis test with Dunn's multiple comparisons test was performed. For comparisons over a time course, a 2-way ANOVA was employed with the Geisser-Greenhouse correction and the Tukey test to correct for multiple comparisons (Sidak's test was used for comparing only two groups over a dilution series). For T cell assays a mixed-effect model with the Geisser-Greenhouse correction and a Tukey test was used, as not all samples were available at each time point. For comparisons of viral load in NHP and viral load and weight loss in hamsters over time, a 2-way ANOVA was employed with the Geisser-Greenhouse correction and a Dunnett test to correct for multiple comparisons, with comparisons to the PBS control group only. For comparisons of NHP titers post-challenge over time (not all samples were available at the last time point), a mixed-effect model was employed with the Geisser-Greenhouse correction and a Dunnett test, with comparisons controlled to the

626 week 5 time point. For the weight loss versus binding titer correlation, a Spearman correlation test was

627 performed. All binding titer and viral load data were log-transformed before performing statistical tests.

628

Author Contributions

JRF, KSC, RAS, MGL, VL, TB, TMF, DC, RC, CG, MK, RvdM contributed to the concept or design of the study. JRF, BJF, KEF, ATN, APW, INM, MG, TSJ, CT, RLD, BF, SOC, SFA, EL, DRF, STN, MMD, ALZ, CA, SF, MJG, SS, VVE, KF, LL, HA, AC, AA, LP, and AVR collected and analyzed data. JPMT, AT, and EMC provided study coordination. ITT, TZ and DL contributed critical reagents. JRF, RAS, CB, SR were involved in the analysis and interpretation of the data. BFH, RAS, MSS, GA, MR, PDK, NJS, DCD, BSG provided supervision. All authors had full access to the data and approved the manuscript before it was submitted by the corresponding author

Declaration of interests

All authors have declared the following interests:

VL, TB, CB, SR, TMF, DC, RC are Sanofi Pasteur employees and may hold stock.

MK, RvdM, and CG are employees of the GSK group of companies and report ownership of GSK shares.

Acknowledgement

The authors thank Jon Smith for coordinating the production and providing the vaccine antigens for the study, and Chris Case for project management.

Funding statement

Funding was provided in part by the National Institutes of Health intramural research program, Sanofi Pasteur, and the US Government through Biomedical Advanced Research and Development Authority (BARDA) under contract HHSO100201600005I.

Figure 1. Vaccine design and study outline.
a, Schematic of the SARS-CoV-2 spike protein, preS dTM, with stabilizing mutations at the S1/S2 furin cleavage site and the heptad repeat region; the transmembrane domain was replaced with a T4 trimerization domain. **b**, Schematic of NHP immunogenicity and challenge study. Immunizations were given at study weeks 0, 3; challenge was performed at study week 6; blood draws approximated by red droplets; PCR and necropsy/histopathology approximated by arrows.

Figure 2. Serology following vaccination with AS03-adjuvanted preS dTM.
Rhesus macaques were immunized with 4 or 12 μg of preS dTM adjuvanted with AS03 adjuvant at weeks 0 and 3. **a**, Endpoint binding titers following pre-vaccination (week 0) or post prime (week 2) and boost (week 5). **b,** Binding titers to the S1 domain, N-terminal domain (RBD) or receptor binding domain (RBD) at week 5. **c**, Avidity index at weeks 2 and 5. **d**, Plasma inhibition of ACE2 binding to spike; week 5 vaccine dose response at 1:40 dilution (left graph) or over multiple dilutions (right graph) are shown. Dotted lines indicate upper and lower limits of quantitation. **e**, Pseudovirus neutralization over time; IC_{50} values are plotted. **f**, Live virus neutralization over time; IC_{50} values are plotted. Symbols represent individual animals; box plots indicate the median and interquartile range; whiskers indicate minimum and maximum data points. Geometric mean values for binding and neutralization are indicated in tables below each graph. Two human convalescent serum (HCS) panels are plotted for comparison. Asterisks indicate significance compared to the PBS control group as follows: *, $p<0.05$; **, $p<0.01$; ***, $p<0.001$ ****, $p<0.0001$.

Figure 3. T cell responses following vaccination with AS03-adjuvanted preS dTM.
T cell responses in rhesus macaques immunized with 4 or 12 ug of preS dTM adjuvanted with AS03 adjuvant at weeks 0 and 3. Cells taken before immunization (prevax) or at week 5 were stimulated with the S1 peptide pool covering the spike protein, then assessed by intracellular cytokine staining. **a**, Percent of memory CD4 T cells expressing any T_H1 cytokine (IL-2, TNF, or IFNγ; left graph), or any T_H2 cytokine (IL-4 or IL-13; right graph). **b**, Percent of memory CD4 T cells expressing the indicated cytokine. **c**, Percent of CD4 T cells expressing the T_{FH} markers IL-21 (left graphs) or CD40L (right graphs) in all memory CD4 cells (top row) or the T_{FH} subset (bottom row). **d**, Proportion of memory CD4 T cells expressing any T_H1 (IL-2, TNF, or IFNγ), T_H2 (IL-4 or IL-13), or T_{FH} (IL-21 or CD40L) markers by ICS Boolean gating; week 5 responses from both vaccine dose groups are averaged. Pie arcs indicate the proportion of cells expressing any T_H1 and T_H2 cytokines in the same cell (brown arc); T_H1 cytokines only (grey arc), or T_H2 cytokines only (pink arc). **e**, Percent of memory CD8 T cells expressing any T_H1 cytokine (IL-2, TNF, or IFNγ). Symbols represent individual animals; box plots indicate the median and interquartile range; whiskers indicate minimum and maximum data points. Asterisks indicate significance compared to the PBS control group (unless otherwise indicated) as follows: *, $p<0.05$; **, $p<0.01$; ***, $p<0.001$ ****, $p<0.0001$.

Figure 4. Vaccination with AS03-adjuvanted preS dTM protects NHP from SARS-CoV-2 challenge.
Rhesus macaques immunized with 4 or 12 μg of AS03-adjuvanted preS dTM were challenged with $3x10^6$ PFU SARS-CoV-2 by the intranasal and intratracheal routes. SARS-CoV-2 subgenomic RNA (sgRNA) in BAL (**a**) and nasal swabs (**b**) at 2, 4, and 7 days following challenge. Symbols represent individual animals; bars indicate group geometric means. Dotted lines indicate lower limit of quantitation. (**C**) Histopathological analysis at 7 days post challenge. Representative images from lung sections from 2 animals per group analyzed by H&E stain for inflammation (top row, 4x magnification), or immunohistochemical (IHC) staining for viral antigen (middle row, 4x magnification; bottom row, 10x magnification). Red arrows indicate foci of viral antigen. **d-f**, Quantification of histopathology for 4 animals at days 7, 8 post challenge. Inflammation from H&E staining, **d**; viral antigen from IHC, **e**; and eosinophils from IHC, **f**. Symbols represent individual animals; box plots indicate the median and interquartile range; whiskers indicate minimum and maximum data points. Asterisks indicate significance compared to the PBS control group as follows: *, $p<0.05$; **, $p<0.01$; ****, $p<0.0001$.

Figure 5. Anamnestic antibody responses in the lung following SARS-CoV-2 challenge. Bronchoalveolar lavage (BAL) supernatant was collected prior to challenge (week 5) and on days 2, 4, 7 and 14 following SARS-CoV-2 challenge. S-2P IgG (**a**) and IgA (**b**) binding titers in BAL samples. S-2P IgG binding titers in nasal washes (**c**) and plasma (**d**) taken pre- and post- challenge. Symbols represent individual animals; box plots indicate the median and interquartile range; whiskers indicate minimum and maximum data points. Asterisks indicate significance compared to the PBS control group as follows: *, $p<0.05$; **, $p<0.01$; ***, $p<0.001$.

Figure 6. Passively transferred IgG from vaccinated NHP protects hamsters. Total IgG was isolated from pooled week 6 sera from rhesus macaques immunized with 3 μg of AS03-adjuvanted preS dTM. 10 or 2 mg total IgG was transferred to hamsters; 10 mg IgG from before (pre-) vaccination or PBS was transferred as a negative control for protection; 10 mg/kg mAb 555 was transferred as a positive control. Animals were then challenged 1 day later with SARS-CoV-2; body weight was recorded daily and oral swabs were taken for PCR on days 2, 4 and 7. **a**, Passive transfer study timeline. **b**, Daily change in body weight following challenge. Lines depict group mean body weight change from day 0; error bars represent SEM. **c**, Correlation between serum S-2P binding titer and percent weight loss on day 6 following SARS-CoV-2 challenge. Curve depicts a 4-parameter logistic fit of the data. Symbols represent individual animals; box plots indicate the median and interquartile range; whiskers indicate minimum and maximum data points. Asterisks indicate significance compared to the PBS control group at each time point: *, $p<0.05$; **, $p<0.01$; ***, $p<0.001$.

727 References
728
729
730 1. Johns Hopkins University. Coronavirus (COVID-19) Information and Updates. [cited]Available
731 from: https://www.coronavirustraining.org/live-map.
732
733 2. Haynes, B.F. *et al.* Prospects for a safe COVID-19 vaccine. *Sci Transl Med* (2020).
734
735 3. Jackson, L.A. *et al.* An mRNA Vaccine against SARS-CoV-2 - Preliminary Report. *N Engl J*
736 *Med* **383**, 1920-1931 (2020).
737
738 4. Polack, F.P. *et al.* Safety and Efficacy of the BNT162b2 mRNA Covid-19 Vaccine. *N Engl J Med*
739 **383**, 2603-2615 (2020).
740
741 5. Voysey, M. *et al.* Safety and efficacy of the ChAdOx1 nCoV-19 vaccine (AZD1222) against
742 SARS-CoV-2: an interim analysis of four randomised controlled trials in Brazil, South Africa,
743 and the UK. *Lancet* **397**, 99-111 (2021).
744
745 6. Logunov, D.Y. *et al.* Safety and immunogenicity of an rAd26 and rAd5 vector-based
746 heterologous prime-boost COVID-19 vaccine in two formulations: two open, non-randomised
747 phase 1/2 studies from Russia. *Lancet* **396**, 887-897 (2020).
748
749 7. Zhang, Y. *et al.* Safety, tolerability, and immunogenicity of an inactivated SARS-CoV-2 vaccine
750 in healthy adults aged 18-59 years: a randomised, double-blind, placebo-controlled, phase 1/2
751 clinical trial. *Lancet Infect Dis* (2020).
752
753 8. WHO. DRAFT landscape of COVID-19 candidate vaccines. [cited 2020 29 October
754 2020]Available from: https://www.who.int/publications/m/item/draft-landscape-of-covid-19-
755 candidate-vaccines
756
757 9. Gao, Q. *et al.* Development of an inactivated vaccine candidate for SARS-CoV-2. *Science* **369**,
758 77-81 (2020).
759
760 10. Wang, H. *et al.* Development of an Inactivated Vaccine Candidate, BBIBP-CorV, with Potent
761 Protection against SARS-CoV-2. *Cell* **182**, 713-721 e719 (2020).
762
763 11. Li, F. Structure, Function, and Evolution of Coronavirus Spike Proteins. *Annu Rev Virol* **3**, 237-
764 261 (2016).
765
766 12. Hoffmann, M. *et al.* SARS-CoV-2 Cell Entry Depends on ACE2 and TMPRSS2 and Is Blocked
767 by a Clinically Proven Protease Inhibitor. *Cell* **181**, 271-280 e278 (2020).
768
769 13. Bosch, B.J., van der Zee, R., de Haan, C.A. & Rottier, P.J. The coronavirus spike protein is a
770 class I virus fusion protein: structural and functional characterization of the fusion core complex.
771 *J Virol* **77**, 8801-8811 (2003).
772
773 14. Walls, A.C. *et al.* Tectonic conformational changes of a coronavirus spike glycoprotein promote
774 membrane fusion. *Proc Natl Acad Sci U S A* **114**, 11157-11162 (2017).
775
776 15. Joyce, M.G. *et al.* A Cryptic Site of Vulnerability on the Receptor Binding Domain of the SARS-
777 CoV-2 Spike Glycoprotein. *bioRxiv* (2020).

16. Rogers, T.F. *et al.* Isolation of potent SARS-CoV-2 neutralizing antibodies and protection from disease in a small animal model. *Science* **369**, 956-963 (2020).

17. Noy-Porat, T. *et al.* A panel of human neutralizing mAbs targeting SARS-CoV-2 spike at multiple epitopes. *Nat Commun* **11**, 4303 (2020).

18. Baum, A. *et al.* REGN-COV2 antibodies prevent and treat SARS-CoV-2 infection in rhesus macaques and hamsters. *Science* (2020).

19. Zost, S.J. *et al.* Potently neutralizing and protective human antibodies against SARS-CoV-2. *Nature* **584**, 443-449 (2020).

20. Liu, L. *et al.* Potent neutralizing antibodies against multiple epitopes on SARS-CoV-2 spike. *Nature* **584**, 450-456 (2020).

21. Chi, X. *et al.* A neutralizing human antibody binds to the N-terminal domain of the Spike protein of SARS-CoV-2. *Science* **369**, 650-655 (2020).

22. Pallesen, J. *et al.* Immunogenicity and structures of a rationally designed prefusion MERS-CoV spike antigen. *Proc Natl Acad Sci U S A* **114**, E7348-E7357 (2017).

23. Kirchdoerfer, R.N. *et al.* Stabilized coronavirus spikes are resistant to conformational changes induced by receptor recognition or proteolysis. *Sci Rep* **8**, 15701 (2018).

24. Wrapp, D. *et al.* Cryo-EM structure of the 2019-nCoV spike in the prefusion conformation. *Science* **367**, 1260-1263 (2020).

25. Mercado, N.B. *et al.* Single-shot Ad26 vaccine protects against SARS-CoV-2 in rhesus macaques. *Nature* **586**, 583-588 (2020).

26. Keech, C. *et al.* Phase 1-2 Trial of a SARS-CoV-2 Recombinant Spike Protein Nanoparticle Vaccine. *N Engl J Med* (2020).

27. Jackson, L.A. *et al.* An mRNA Vaccine against SARS-CoV-2 - Preliminary Report. *N Engl J Med* (2020).

28. Corbett, K.S. *et al.* Evaluation of the mRNA-1273 Vaccine against SARS-CoV-2 in Nonhuman Primates. *N Engl J Med* **383**, 1544-1555 (2020).

29. Walsh, E.E. *et al.* Safety and Immunogenicity of Two RNA-Based Covid-19 Vaccine Candidates. *N Engl J Med* (2020).

30. Cunningham, A.L. *et al.* Efficacy of the Herpes Zoster Subunit Vaccine in Adults 70 Years of Age or Older. *N Engl J Med* **375**, 1019-1032 (2016).

31. Wheeler, C.M. *et al.* Efficacy, safety, and immunogenicity of the human papillomavirus 16/18 AS04-adjuvanted vaccine in women older than 25 years: 7-year follow-up of the phase 3, double-blind, randomised controlled VIVIANE study. *Lancet Infect Dis* **16**, 1154-1168 (2016).

32. Chen, D.S. Hepatitis B vaccination: The key towards elimination and eradication of hepatitis B. *J Hepatol* **50**, 805-816 (2009).

33. Coffman, R.L., Sher, A. & Seder, R.A. Vaccine adjuvants: putting innate immunity to work. *Immunity* **33**, 492-503 (2010).

34. Ellebedy, A.H. *et al.* Adjuvanted H5N1 influenza vaccine enhances both cross-reactive memory B cell and strain-specific naive B cell responses in humans. *Proc Natl Acad Sci U S A* **117**, 17957-17964 (2020).

35. Leroux-Roels, I. *et al.* Antigen sparing and cross-reactive immunity with an adjuvanted rH5N1 prototype pandemic influenza vaccine: a randomised controlled trial. *Lancet* **370**, 580-589 (2007).

36. Khurana, S. *et al.* AS03-adjuvanted H5N1 vaccine promotes antibody diversity and affinity maturation, NAI titers, cross-clade H5N1 neutralization, but not H1N1 cross-subtype neutralization. *NPJ Vaccines* **3**, 40 (2018).

37. Nachbagauer, R. *et al.* A chimeric haemagglutinin-based influenza split virion vaccine adjuvanted with AS03 induces protective stalk-reactive antibodies in mice. *NPJ Vaccines* **1** (2016).

38. Chen, W.H. *et al.* Persistence of Antibody to Influenza A/H5N1 Vaccine Virus: Impact of AS03 Adjuvant. *Clin Vaccine Immunol* **23**, 73-77 (2016).

39. Leroux-Roels, I. *et al.* Priming with AS03 A-adjuvanted H5N1 influenza vaccine improves the kinetics, magnitude and durability of the immune response after a heterologous booster vaccination: an open non-randomised extension of a double-blind randomised primary study. *Vaccine* **28**, 849-857 (2010).

40. Schwarz, T.F. *et al.* Single dose vaccination with AS03-adjuvanted H5N1 vaccines in a randomized trial induces strong and broad immune responsiveness to booster vaccination in adults. *Vaccine* **27**, 6284-6290 (2009).

41. Cohet, C. *et al.* Safety of AS03-adjuvanted influenza vaccines: A review of the evidence. *Vaccine* **37**, 3006-3021 (2019).

42. Guebre-Xabier, M. *et al.* NVX-CoV2373 vaccine protects cynomolgus macaque upper and lower airways against SARS-CoV-2 challenge. *Vaccine* **38**, 7892-7896 (2020).

43. van Doremalen, N. *et al.* ChAdOx1 nCoV-19 vaccine prevents SARS-CoV-2 pneumonia in rhesus macaques. *Nature* **586**, 578-582 (2020).

44. Tao, Y., Strelkov, S.V., Mesyanzhinov, V.V. & Rossmann, M.G. Structure of bacteriophage T4 fibritin: a segmented coiled coil and the role of the C-terminal domain. *Structure* **5**, 789-798 (1997).

45. Lu, Y., Welsh, J.P. & Swartz, J.R. Production and stabilization of the trimeric influenza hemagglutinin stem domain for potentially broadly protective influenza vaccines. *Proc Natl Acad Sci U S A* **111**, 125-130 (2014).

46. Miner, K.T. & Croft, M. Generation, persistence, and modulation of Th0 effector cells: role of autocrine IL-4 and IFN-gamma. *J Immunol* **160**, 5280-5287 (1998).

47. Firestein, G.S. *et al.* A new murine CD4+ T cell subset with an unrestricted cytokine profile. *J Immunol* **143**, 518-525 (1989).

48. Annette B. Vogel, I.K., Ye Che, Kena A. Swanson, Alexander Muik, Mathias Vormehr, Lena M. Kranz, Kerstin C. Walzer, Stephanie Hein, Alptekin Güler, Jakob Loschko, Mohan S. Maddur, Kristin Tompkins, Journey Cole, Bonny G. Lui, Thomas Ziegenhals, Arianne Plaschke, David Eisel, Sarah C. Dany, Stephanie Fesser, Stephanie Erbar, Ferdia Bates, Diana Schneider, Bernadette Jesionek, Bianca Sänger, Ann-Kathrin Wallisch, Yvonne Feuchter, Hanna Junginger, Stefanie A. Krumm, André P. Heinen, Petra Adams-Quack, Julia Schlereth, Christoph Kröner, Shannan Hall-Ursone, Kathleen Brasky, Matthew C. Griffor, Seungil Han, Joshua A. Lees, Ellene H. Mashalidis, Parag V. Sahasrabudhe, Charles Y. Tan, Danka Pavliakova, Guy Singh, Camila Fontes-Garfias, Michael Pride, Ingrid L. Scully, Tara Ciolino, Jennifer Obregon, Michal Gazi, Ricardo Carrion Jr., Kendra J. Alfson, Warren V. Kalina, Deepak Kaushal, Pei-Yong Shi, Thorsten Klamp, Corinna Rosenbaum, Andreas N. Kuhn, Özlem Türeci, Philip R. Dormitzer, Kathrin U. Jansen, Ugur Sahin. A prefusion SARS-CoV-2 spike RNA vaccine is highly immunogenic and prevents lung infection in non-human primates. *bioRxiv* (2020).

49. V'Kovski, P., Kratzel, A., Steiner, S., Stalder, H. & Thiel, V. Coronavirus biology and replication: implications for SARS-CoV-2. *Nat Rev Microbiol* (2020).

50. Jones, B.E. *et al.* LY-CoV555, a rapidly isolated potent neutralizing antibody, provides protection in a non-human primate model of SARS-CoV-2 infection. *bioRxiv* (2020).

51. Yam, K.K. *et al.* AS03-Adjuvanted, Very-Low-Dose Influenza Vaccines Induce Distinctive Immune Responses Compared to Unadjuvanted High-Dose Vaccines in BALB/c Mice. *Front Immunol* **6**, 207 (2015).

52. Madan, A. *et al.* Immunogenicity and Safety of an AS03-Adjuvanted H7N9 Pandemic Influenza Vaccine in a Randomized Trial in Healthy Adults. *J Infect Dis* **214**, 1717-1727 (2016).

53. Zheng, Y. *et al.* Respiratory Syncytial Virus F Subunit Vaccine With AS02 Adjuvant Elicits Balanced, Robust Humoral and Cellular Immunity in BALB/c Mice. *Front Immunol* **11**, 526965 (2020).

54. Baz, M. *et al.* Effects of different adjuvants in the context of intramuscular and intranasal routes on humoral and cellular immune responses induced by detergent-split A/H3N2 influenza vaccines in mice. *Clin Vaccine Immunol* **19**, 209-218 (2012).

55. Leroux-Roels, G. *et al.* Impact of adjuvants on CD4(+) T cell and B cell responses to a protein antigen vaccine: Results from a phase II, randomized, multicenter trial. *Clin Immunol* **169**, 16-27 (2016).

56. Moris, P. *et al.* H5N1 influenza vaccine formulated with AS03 A induces strong cross-reactive and polyfunctional CD4 T-cell responses. *J Clin Immunol* **31**, 443-454 (2011).

57. Richmond, P. *et al.* Safety and immunogenicity of S-Trimer (SCB-2019), a protein subunit vaccine candidate for COVID-19 in healthy adults: a phase 1, randomised, double-blind, placebo-controlled trial. *Lancet* (2021).

58. Delgado, M.F. *et al.* Lack of antibody affinity maturation due to poor Toll-like receptor stimulation leads to enhanced respiratory syncytial virus disease. *Nat Med* **15**, 34-41 (2009).

59. Graham, B.S. *et al.* Priming immunization determines T helper cytokine mRNA expression patterns in lungs of mice challenged with respiratory syncytial virus. *J Immunol* **151**, 2032-2040 (1993).

60. De Swart, R.L. *et al.* Immunization of macaques with formalin-inactivated respiratory syncytial virus (RSV) induces interleukin-13-associated hypersensitivity to subsequent RSV infection. *J Virol* **76**, 11561-11569 (2002).

61. Philip R. Nader, M.S.H., John Rousseau. Atypical exanthem following exposure to natural measles: Eleven cases in children previously inoculated with killed vaccine. *The Journal of Pediatrics* **72**, 22-28 (1968).

62. Chin, J., Magoffin, R.L., Shearer, L.A., Schieble, J.H. & Lennette, E.H. Field evaluation of a respiratory syncytial virus vaccine and a trivalent parainfluenza virus vaccine in a pediatric population. *Am J Epidemiol* **89**, 449-463 (1969).

63. Tseng, C.T. *et al.* Immunization with SARS coronavirus vaccines leads to pulmonary immunopathology on challenge with the SARS virus. *PLoS One* **7**, e35421 (2012).

64. Murphy, B.R. *et al.* Dissociation between serum neutralizing and glycoprotein antibody responses of infants and children who received inactivated respiratory syncytial virus vaccine. *J Clin Microbiol* **24**, 197-202 (1986).

65. Murphy, B.R. & Walsh, E.E. Formalin-inactivated respiratory syncytial virus vaccine induces antibodies to the fusion glycoprotein that are deficient in fusion-inhibiting activity. *J Clin Microbiol* **26**, 1595-1597 (1988).

66. Yu, J. *et al.* DNA vaccine protection against SARS-CoV-2 in rhesus macaques. *Science* **369**, 806-811 (2020).

67. Chan, J.F. *et al.* Simulation of the Clinical and Pathological Manifestations of Coronavirus Disease 2019 (COVID-19) in a Golden Syrian Hamster Model: Implications for Disease Pathogenesis and Transmissibility. *Clin Infect Dis* **71**, 2428-2446 (2020).

68. McMahan, K. *et al.* Correlates of protection against SARS-CoV-2 in rhesus macaques. *Nature* (2020).

69. Adenyi-Jones, S.C., Faden, H., Ferdon, M.B., Kwong, M.S. & Ogra, P.L. Systemic and local immune responses to enhanced-potency inactivated poliovirus vaccine in premature and term infants. *J Pediatr* **120**, 686-689 (1992).

70. Zhaori, G., Sun, M. & Ogra, P.L. Characteristics of the immune response to poliovirus virion polypeptides after immunization with live or inactivated polio vaccines. *J Infect Dis* **158**, 160-165 (1988).

71. Ogra, P.L., Karzon, D.T., Righthand, F. & MacGillivray, M. Immunoglobulin response in serum and secretions after immunization with live and inactivated poliovaccine and natural infection. *N Engl J Med* **279**, 893-900 (1968).

72. Vujanic, A. *et al.* Long-term antibody and immune memory response induced by pulmonary delivery of the influenza Iscomatrix vaccine. *Clin Vaccine Immunol* **19**, 79-83 (2012).

73. Sealy, R., Webby, R.J., Crumpton, J.C. & Hurwitz, J.L. Differential localization and function of antibody-forming cells responsive to inactivated or live-attenuated influenza virus vaccines. *Int Immunol* **25**, 183-195 (2013).

74. Matsuoka, T. *et al.* Characteristics of immunity induced by viral antigen or conferred by antibody via different administration routes. *Clin Exp Immunol* **130**, 386-392 (2002).

75. Salisch, N.C. *et al.* Adenovectors encoding RSV-F protein induce durable and mucosal immunity in macaques after two intramuscular administrations. *NPJ Vaccines* **4**, 54 (2019).

76. Sterlin, D. *et al.* IgA dominates the early neutralizing antibody response to SARS-CoV-2. *Sci Transl Med* (2020).

77. Diebold, S.S., Kaisho, T., Hemmi, H., Akira, S. & Reis e Sousa, C. Innate antiviral responses by means of TLR7-mediated recognition of single-stranded RNA. *Science* **303**, 1529-1531 (2004).

78. Garcon, N., Vaughn, D.W. & Didierlaurent, A.M. Development and evaluation of AS03, an Adjuvant System containing alpha-tocopherol and squalene in an oil-in-water emulsion. *Expert Rev Vaccines* **11**, 349-366 (2012).

79. Zhou, T. *et al.* Structure-Based Design with Tag-Based Purification and In-Process Biotinylation Enable Streamlined Development of SARS-CoV-2 Spike Molecular Probes. *Cell Rep* **33**, 108322 (2020).

80. Wang, L. *et al.* Evaluation of candidate vaccine approaches for MERS-CoV. *Nat Commun* **6**, 7712 (2015).

81. Bottcher, E. *et al.* Proteolytic activation of influenza viruses by serine proteases TMPRSS2 and HAT from human airway epithelium. *J Virol* **80**, 9896-9898 (2006).

82. Vanderheiden, A. *et al.* Development of a Rapid Focus Reduction Neutralization Test Assay for Measuring SARS-CoV-2 Neutralizing Antibodies. *Curr Protoc Immunol* **131**, e116 (2020).

83. Xie, X. *et al.* An Infectious cDNA Clone of SARS-CoV-2. *Cell Host Microbe* **27**, 841-848 e843 (2020).

84. Katzelnick, L.C. *et al.* Viridot: An automated virus plaque (immunofocus) counter for the measurement of serological neutralizing responses with application to dengue virus. *PLoS Negl Trop Dis* **12**, e0006862 (2018).

85. Beddall, M., Chattopadhyay, P.K., Kao, S.F., Foulds, K. & Roederer, M. A simple tube adapter to expedite and automate thawing of viably frozen cells. *J Immunol Methods* **439**, 74-78 (2016).

86. Donaldson, M.M., Kao, S.F. & Foulds, K.E. OMIP-052: An 18-Color Panel for Measuring Th1, Th2, Th17, and Tfh Responses in Rhesus Macaques. *Cytometry A* **95**, 261-263 (2019).

87. Brown, E.P. *et al.* High-throughput, multiplexed IgG subclassing of antigen-specific antibodies from clinical samples. *J Immunol Methods* **386**, 117-123 (2012).

88. Ackerman, M.E. *et al.* A robust, high-throughput assay to determine the phagocytic activity of clinical antibody samples. *J Immunol Methods* **366**, 8-19 (2011).

89. Fischinger, S. *et al.* A high-throughput, bead-based, antigen-specific assay to assess the ability of antibodies to induce complement activation. *J Immunol Methods* **473**, 112630 (2019).

90. Karsten, C.B. *et al.* A versatile high-throughput assay to characterize antibody-mediated neutrophil phagocytosis. *J Immunol Methods* **471**, 46-56 (2019).

91. Lu, L.L. *et al.* A Functional Role for Antibodies in Tuberculosis. *Cell* **167**, 433-443 e414 (2016).

a

SARS-CoV-2 Immunogen Design

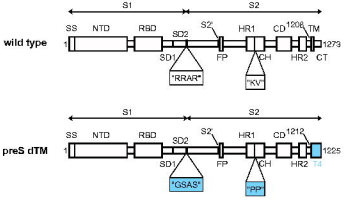

b

NHP Immunogenicity Study Timeline

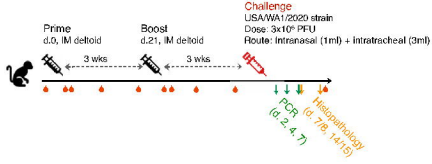

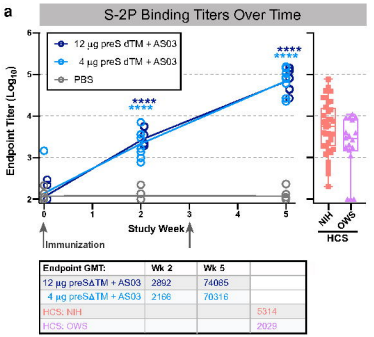

Endpoint GMT:	Wk 2	Wk 5	
12 µg preSΔTM + AS03	2892	74085	
4 µg preSΔTM + AS03	2166	70316	
HCS: NIH			5314
HCS: OWS			2029

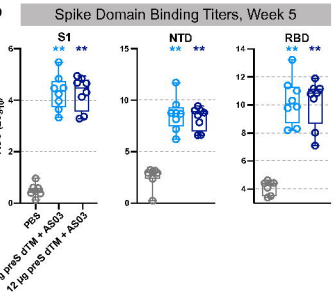

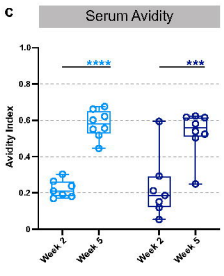

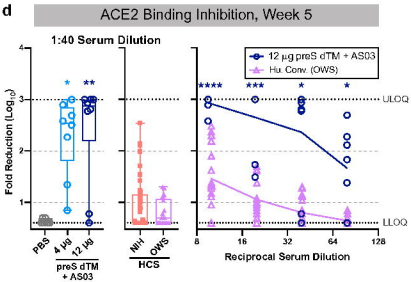

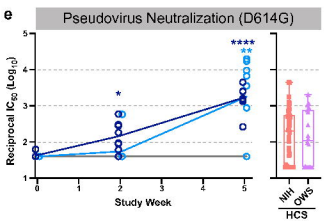

IC50 GMT:	Wk 2	Wk 5	
12 µg preS dTM + AS03	145	1667	
4 µg preS dTM + AS03	56	1798	
HCS: NIH			152
HCS: OWS			123

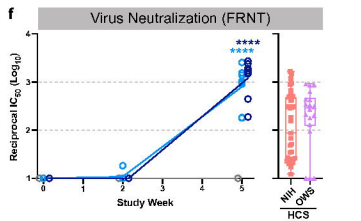

IC50 GMT:	Wk 2	Wk 5	
12 µg preS dTM + AS03	10	1200	
4 µg preS dTM + AS03	11	801	
HCS: NIH			116
HCS: OWS			186

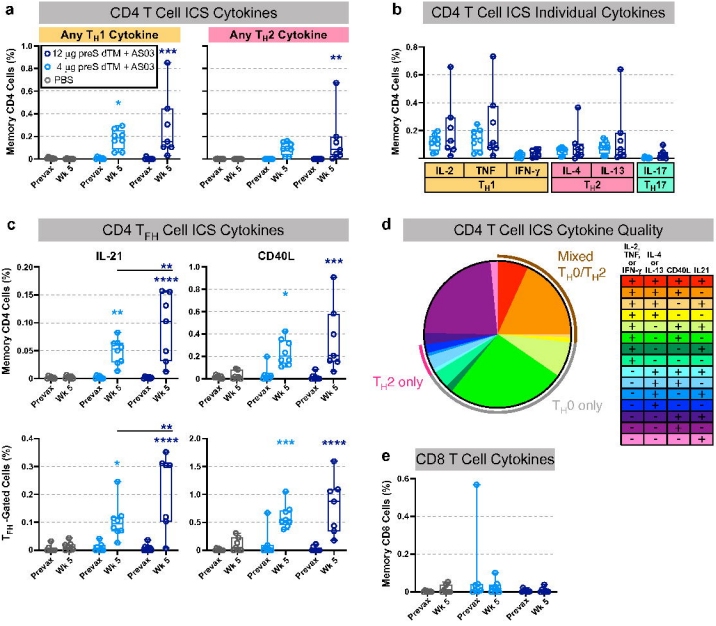
a
CD4 T Cell ICS Cytokines
Any TH1 Cytokine
Any TH2 Cytokine
12 μg preS dTM + AS03
4 μg preS dTM + AS03
PBS
Memory CD4 Cells (%)
Prevax
Wk 5
b
CD4 T Cell ICS Individual Cytokines
Memory CD4 Cells (%)
IL-2
TNF
IFN-γ
IL-4
IL-13
IL-17
TH1
TH2
TH17
c
CD4 TFH Cell ICS Cytokines
IL-21
CD40L
Memory CD4 Cells (%)
TH-Gated Cells (%)
d
CD4 T Cell ICS Cytokine Quality
Mixed TH0/TH2
TH2 only
TH0 only
IL-2, TNF, IFN-γ
IL-4 or IL-13
CD40L
IL21
e
CD8 T Cell Cytokines
Memory CD8 Cells (%)

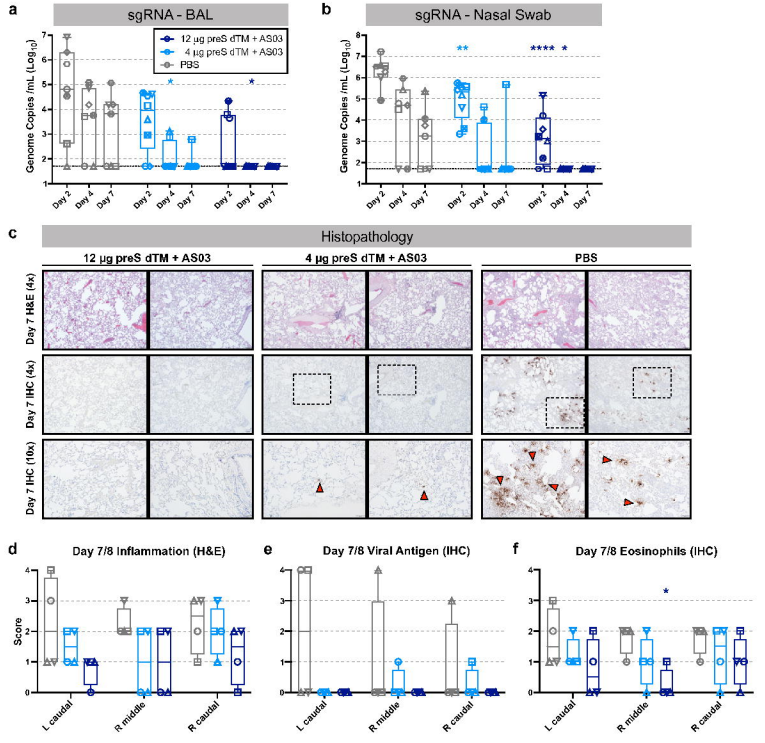
a
sgRNA - BAL
12 µg preS dTM + AS03
4 µg preS dTM + AS03
PBS
Genome Copies /mL (Log10)
Day 2
Day 4
Day 7
b
sgRNA - Nasal Swab
c
Histopathology
12 µg preS dTM + AS03
4 µg preS dTM + AS03
PBS
Day 7 H&E (4x)
Day 7 IHC (4x)
Day 7 IHC (10x)
d
Day 7/8 Inflammation (H&E)
Score
L caudal
R middle
R caudal
e
Day 7/8 Viral Antigen (IHC)
f
Day 7/8 Eosinophils (IHC)

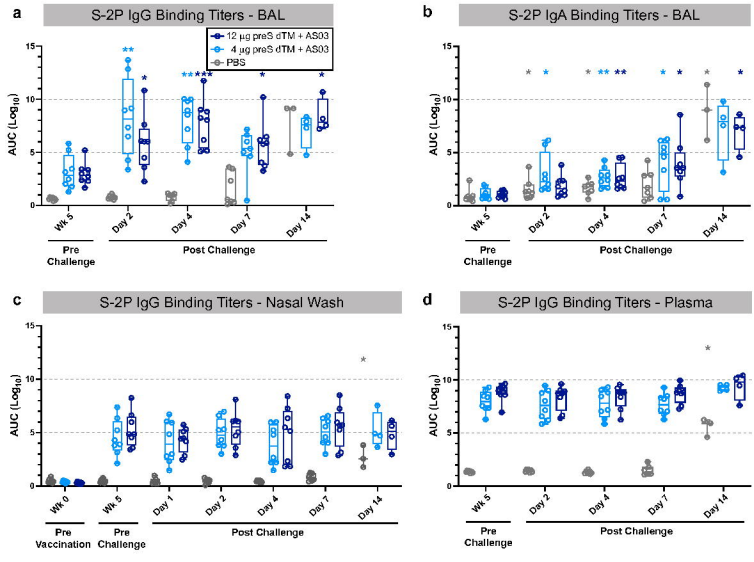
a
S-2P IgG Binding Titers - BAL
12 µg preS dTM + AS03
4 µg preS dTM + AS03
PBS
AUC (Log10)
Wk 5
Day 2
Day 4
Day 7
Day 14
Pre Challenge
Post Challenge
b
S-2P IgA Binding Titers - BAL
AUC (Log10)
Wk 5
Day 2
Day 4
Day 7
Day 14
Pre Challenge
Post Challenge
c
S-2P IgG Binding Titers - Nasal Wash
AUC (Log10)
Wk 0
Wk 5
Day 1
Day 2
Day 4
Day 7
Day 14
Pre Vaccination
Pre Challenge
Post Challenge
d
S-2P IgG Binding Titers - Plasma
AUC (Log10)
Wk 5
Day 2
Day 4
Day 7
Day 14
Pre Challenge
Post Challenge

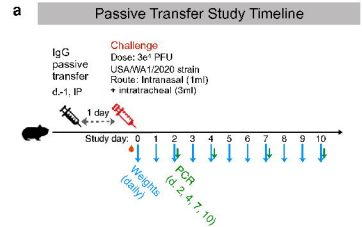
a
Passive Transfer Study Timeline
IgG passive transfer d.-1, IP
Challenge
Dose: 3e4 PFU
USA/WA1/2020 strain
Route: Intranasal (1ml) + intratracheal (3ml)
1 day
Study day: 0 1 2 3 4 5 6 7 8 9 10
Weights (daily)
POR (d. 2, 4, 7, 10)

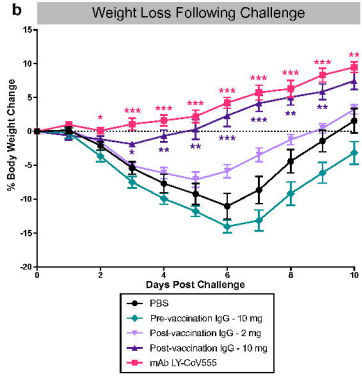
b
Weight Loss Following Challenge
% Body Weight Change
Days Post Challenge
PBS
Pre-vaccination IgG - 10 mg
Post-vaccination IgG - 2 mg
Post-vaccination IgG - 10 mg
mAb LY-CoV555

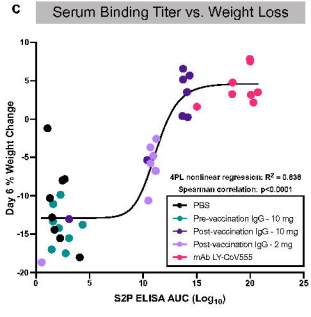
c
Serum Binding Titer vs. Weight Loss
Day 6 % Weight Change
S2P ELISA AUC (Log10)
4PL nonlinear regression: R2 = 0.838
Spearman correlation: p<0.0001
PBS
Pre-vaccination IgG - 10 mg
Post-vaccination IgG - 10 mg
Post-vaccination IgG - 2 mg
mAb LY-CoV555